



Arrhenius Plot Analysis, Temperature Coefficient and Q₁₀ Value Estimation for the Effect of Temperature on the Rate of Molybdenum Reduction by *Acinetobacter calcoaceticus* strain Dr Y12

Abubakar Aisami¹*

¹Department of Biochemistry, Faculty of Science, Gombe State University, Nigeria.

*Corresponding author:

Abubakar Aisami

Department of Biochemistry, Faculty of Science,
Gombe State University,
Nigeria.

Email: abubakar.aisami05@gmail.com

HISTORY

Received: 12th April 2021
Received in revised form: 29th June 2021
Accepted: 17th July 2021

KEYWORDS

molybdenum-reducing
Acinetobacter calcoaceticus strain Dr Y12
temperature
Arrhenius plot
breakpoint

ABSTRACT

Molybdenum is a micronutrient that is required as a co-factor for a variety of hydroxylation and redox transfer activities in both animal and plant physiological processes. The potential of overexposure to interfere with the sperm production and egg formation processes in several species, including fish, is the biggest danger of excessive exposure. Only recently has it been discovered that it can be utilised as a remediation method for molybdenum-reducing bacteria. The effect of temperature on molybdenum reduction is one of the variables to consider. It is possible to use many different models to estimate the growth rate of microbes on various media based on the temperature being utilised. The Arrhenius model is popular because it contains a limited number of parameters. In general, the temperature has an effect on the development and metabolic activity of microorganisms on their substrates. Because microorganisms are so tiny, they are very sensitive to changes in their environment's temperature. Growth on molybdenum by *Acinetobacter calcoaceticus* strain Dr Y12 is described, with a discontinuous chevron-like graph of apparent activation energy with a breakpoint at 32.66 °C. Regression analysis results suggest that in the lower temperature range of 20-30 °C, growth on molybdenum had an activation energy of 66.48 kJ/mol, whereas, at the higher temperature range of 37–45 °C, it had an activation energy of 99.5 kJ/mol. For the examined temperature range (20-30 °C) and (37-45 °C), Q₁₀ values of 2.46 and 3.37 and theta values of 1.09 and 1.13 were obtained, respectively. This study is very useful in predicting the breakdown of molybdenum and the movement of molybdenum during bioremediation.

INTRODUCTION

Our actions are putting our ecosystem in danger right now. Heavily polluting the environment include heavy industry, urbanisation, and agriculture, all of which have increased in tandem with the world's population growth [1–4]. Overexploitation of natural resources, as well as men's ignorance of natural laws, contribute to the escalation of the problem [5–8]. Over the years, the amount of pollution caused by hydrocarbons and metal ions has steadily increased across the globe. Toxic chemicals generated from metals and their compounds have been related to a range of acute and chronic toxicity cases in high-exposure settings such as the workplace and the environment, according to research. Heavy metals may be present in the environment in their natural state. Heavy metal levels have increased significantly in recent years as a consequence of human activities dating back to pre-industrial times, according to the Environmental Protection Agency [9–13]. A large and

indiscriminate release of toxins into the environment is happening in parallel with the increase in population and the intensity of industrial activity. The presence of high quantities of heavy metals over the critical load may have negative consequences for human health and the environment. Metals such as arsenic, cadmium, chromium, cobalt, copper, lead, mercury, molybdenum, nickel, silver, and zinc are toxic in their elemental forms and different combinations, and they are also non-biodegradable in their elemental forms and various combinations. Metal accumulation in the food chain may represent a major threat to the ecosystem as a consequence of their carcinogenic and mutagenic properties, which are associated with metals. Heavy metal contamination has risen to the level of a global public health emergency in recent years, making it imperative to remove them from the environment as soon as possible [14–19].

Molybdenum is an important trace element that acts as a micronutrient and is required as a co-factor for over 50 enzymes. It promotes cellular activity in animal and plant physiology, for example, by catalysing a range of hydroxylation and redox transfer processes [20–25]. With molybdenum's widespread use in the industrial production of ceramics, glass and contact lens solution, metallurgical processes, lubricants, pigment, catalyst, electronic goods, and as colour additives in cosmetics, the dangers to people exposed to its toxicity have also increased [26–32]. It has been reported that an increase in the amount of molybdenum in groundwater in mining sites of up to 0.5 mg/L has been found, which is higher than the World Health Organization (WHO) recommended limit of 0.07 mg/L in drinking water [28]. Animals that have had direct contact with molybdenum via drinking water or while foraging for plants are more likely to exhibit hypocuprosis signs or suffer from molybdenosis after a lengthy period [22].

Microorganisms are especially susceptible to molybdenum breakdown when exposed to high temperatures because of their small size. Physiology is influenced by temperature, which allows organisms to better adapt to their changing environments. When it comes to biodegrading chemicals, the temperature is an essential element to take into consideration. For many years, the Arrhenius model has been widely employed in the study of bacterial growth and rates. It is often used to calculate the apparent activation energy, E_a , which is believed to exist for either growth or decay on various metabolic substrates [33–39].

Although being frequently employed in simulating the temperature impact in a limited temperature range, the Arrhenius model is less often used to larger ranges [40]. For most temperature ranges, the value of ΔH (ΔH^*) is approximately constant. However, for extreme ranges of temperature, this number may diverge three or fourfold depending on the range of temperatures being examined [41]. according to some studies, the model may not be accurate when used across the whole bacterial process temperature [42]. The Arrhenius plot may also display a previously discovered transition which is a rapid change in the activation energy [43]. Arrhenius's model has the fewest parameters, making it relatively universally accepted by researchers [40]. In other words, the Arrhenius models are utilised in understanding how temperature affects bacterial development because of this. The Arrhenius parameter estimate is calculated by drawing a linear regression on the Arrhenius plot. Several years ago, similar research looked at Q_{10} value estimates of Arrhenius plot analysis and the impact of temperature on molybdenum growth done by *Pseudomonas* sp. strain DRYJ7 [44]. another competing model, the Ratkowsky, is also built on the assumption of linear growth, but due to biological foundations, this model suffers from a lack of steady development and exhibits non-linear behaviour [45].

This research showed that there were many possible activation energies for the breakdown of molybdenum by a bacterium, which was previously unknown. It is interesting in terms of concepts, and it will also be extremely helpful in forecasting molybdenum removal and transport during bioremediation.

MATERIALS AND METHODS

The activation energy of growth on molybdenum by *Acinetobacter calcoaceticus* strain Dr Y12

Acinetobacter calcoaceticus strain Dr Y12 was grown and maintained in a low phosphate media (LPM) composed of magnesium sulphate pentahydrate $MgSO_4 \cdot 7H_2O$ (0.05%), disodium molybdate dihydrate $Na_2MoO_4 \cdot 2H_2O$ (0.242 % or 10 mM), glucose (1%), ammonium sulphate $(NH_4)_2SO_4$ (0.3%), sodium chloride NaCl (0.5%), yeast extract (0.5%), and disodium phosphate anhydrous Na_2HPO_4 (0.071% or 5 mM) [46]. Molybdenum reduction rate data from *Acinetobacter calcoaceticus* strain Dr Y12 was then processed as previous [39] by transferring the growth values at each temperature to the natural logarithm and calculating the value of the slope, which is equivalent to a specific growth rate.

The Arrhenius equation [47] is as follows,

$$\mu = Ae^{-\frac{E_a}{RT}} \quad [\text{Eqn. 1}]$$

Where T is the absolute temperature (Kelvin = °C + 273.15), R is the universal gas constant (0.008314 kJ/molK⁻¹), E_a is the activation energy (kJ/mol) and A physically signifies the rate constant at which all the participating molecules possess sufficient energy prior reaction ($E_a = 0$). A linearized form is given via the plot of log-normal growth rate against 1/T and the equation is as follows;

$$\ln \mu = \ln A - \frac{E_a}{R} \cdot \frac{1}{T} \quad [\text{Eqn. 2}]$$

Coefficient of Q_{10} estimation

The Q_{10} value is estimated via the following equation;

$$Q_{10} = e^{\left(\frac{E_a}{R}\right)\left(\frac{10}{T_2 T_1}\right)} \quad [\text{Eqn. 3}]$$

Following rearrangement,

$$\ln Q_{10} = \left(\frac{E_a}{R}\right)\left(\frac{1}{T_1 T_2}\right) \quad [\text{Eqn. 4}]$$

The coefficient of temperature or theta (Θ) value (simplified Arrhenius temperature coefficient) is another important biological constant obtained from the substitution of the obtained values into the reaction rates equation governed by the Q_{10} rule;

$$kT = k20\Theta (T-20) \quad [\text{Eqn. 5}]$$

RESULTS AND DISCUSSION

The effect of temperature on the growth rate of the bacterium on molybdenum shows an increasing growth rate leading to a maximum rate at 30 °C and a decrease of growth rate at higher temperatures (Fig. 1). When plotting $\ln q_m$ versus $1/T$, we got a Chevron-like graph, which showed a discontinuous curve across the entire temperature range (Fig. 2). An interesting finding was the presence of a breakpoint at 32.66 °C. Regression analysis results are shown in Table 1 and Table 2 suggest that in the lower temperature range of 20-30 °C, growth on molybdenum had an activation energy of 66.48 kJ/mol, whereas, at the higher temperature range of 37-45 °C, it had an activation energy of 99.54 kJ/mol. A previous study on the growth rate of *Pseudomonas* sp. strain DrYJ7 between 10 and 20 °C on molybdenum showed activation energy of 14.96 KJ/mol [44], which is much lower.

Activation energy estimated using the Arrhenius model was within the published literature's range of activation energy for various biodegradation of xenobiotics (Table 2). The connections seem to require more energy to break apart. Increasing the temperature uses less energy. Of the many reports on the activation energy calculated from rates of metabolic process at various temperatures, very few works report on the presence of two activation energies opting instead to report for only one activation energy spanning a large range of temperature. Of the reports, two contrasting difference is seen wherein one study, a higher activation energy is reported at higher temperatures compared to a lower range of temperature while in another study, an opposite phenomenon is observed (Table 3). A case in point is the growth of *Bacillus* sp. JF8 on polychlorinated biphenyl (PCB) where the activation energy was 12.1 KJ/mol from 20 to 46 °C and 31.4 KJ/mol from 50 to 70 °C [48]. In another contrasting study, the growth of phenol by *Pseudomonas* sp. AQ5-04 shows activation energy of 38.92 KJ/mol from 15 to 30 °C and 11.34 KJ/mol from 35-45 °C [38].

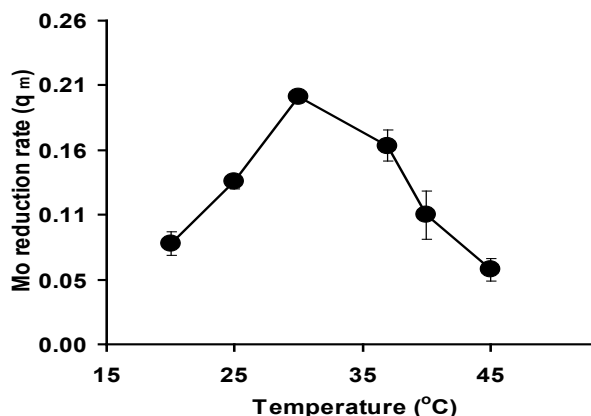


Fig 1. The effect of temperature on the specific growth rate of *Acinetobacter calcoaceticus* strain Dr Y12 on molybdenum. Error bars represent mean ± standard deviation (n=3).

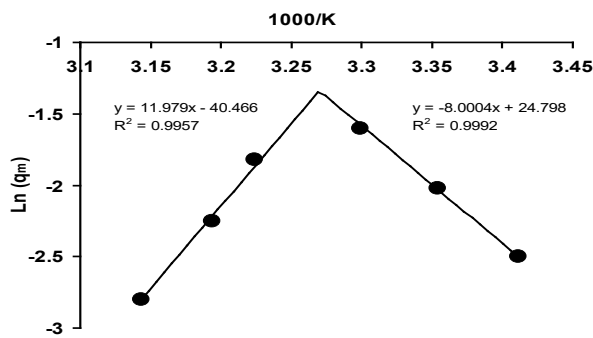


Fig 2. Arrhenius plot of the molybdenum reduction rate by *Acinetobacter calcoaceticus* strain Dr Y12.

Table 1. The two-part linear regression analysis for the Arrhenius plot of molybdenum reduction rate by *Acinetobacter calcoaceticus* strain Dr Y12.

Distribution of the experimental points	Three points to the left, three points to the right
	Right part
Temperature range °C	20,25,30
Regression equation	$y = -8.0004x + 24.798$
Coefficient of determination	0.99
$\tan a \pm$ Standard error	-8.00 ± 0.23
$E_a \pm$ Standard error, kJ mol ⁻¹	66.48 ± 1.91
t-Statistic	-34.73
Degrees of freedom	2
	Left part
Temperature range °C	37,40,45
Regression equation	$y = 11.979x - 40.466$
Coefficient of determination	0.99
$\tan a \pm$ Standard error	11.98 ± 0.79
$E_a \pm$ Standard error, kJ mol ⁻¹	99.54 ± 6.58
t-Statistic	15.13
Degrees of freedom	2
	Breakpoints data
Intersection coordinates, (x, y)	3.27,-1.34
Break point temperature °C	32.66
Q ₁₀ (20-30 °C)	2.46
Theta (20-30 °C)	1.09
Q ₁₀ (37-45 °C)	3.37
Theta (37-45 °C)	1.13

Table 2. Summary of nonlinear regression of the effect of temperature on the rate of molybdenum reduction *Acinetobacter calcoaceticus* strain Dr Y12

Segmental linear regression	
Best-fit values	
intercept1	-39.08
slope1	11.54
X ₀	= 3.270
slope2	-8.236
Std. Error	
intercept1	1.314
slope1	0.4104
slope2	0.3676
95% CI (asymptotic)	
intercept1	-43.26 to -34.90
slope1	10.24 to 12.85
slope2	-9.406 to -7.066
Goodness of Fit	
Degrees of Freedom 3	
R squared	0.9963
Sum of Squares	0.003631
Sy.x	0.03479
Constraints	
X ₀	X ₀ = 3.27

Table 3. Arrhenius temperature characteristics for metal reduction.

Microorganisms	Temperature range (°C)	Substrate	ΔH^* apparent activation energy (kJ.mol ⁻¹)	Ref
<i>Ochrobactrum intermedium</i> BCR400	25-35	Chromate	120.69	[49]
<i>Arthrobacter sp.</i> SUK 1201	25-60	Chromate	36.21	[50]
<i>Aspergillus niger</i>	30-60	Chromate	8.56	[51]
<i>Bacillus sp.</i>	25-40	Chromate	22.0	[52]
<i>Thermus scotoductus</i> SA-01	65	Chromate	35 (membrane bound enzyme)	[53]
<i>Thermus scotoductus</i> SA-01	60-65	Iron	40.3 (soluble)	[53]
<i>Shewanella profunda</i> LT13a	4-37	Iron	30	[54]
<i>β-Proteobacteria</i>	15-40	Vanadate	50.3	[54]
<i>Shewanella oneidensis</i> :MR-1	25-40	Selenate	36	[55]
			Control system 62.90	[56]
			TPPS-supplemented system 47.33	
<i>Acinetobacter calcoaceticus</i> strain Dr.Y12	20-45	Molybdate	66.48 (20-30 °C) 99.54 (37-45 °C)	This study

Note: N(TPPS) Meso-tetrakis (4-sulfonatophenyl) porphyrin mediator

The higher the activation energy, the more energy the bacterium needs to use to metabolize xenobiotics. Based on **Table 3**, the values obtained in this study for both temperature ranges are within the activation energy for numerous metal reductions by microbial species. However, the activation energy for the typical mesophilic bacteria is between 33.5 and 50.3 kJ/mol [57], indicating that the activation energy for one of the temperature range studied in this study was relatively higher. The higher activation energy for the higher range of temperature was within the range reported by the chromate-reducing *Ochrobactrum intermedium* BCR400 [49] (**Table 3**).

In the current study, we found that the activation energy is not constant, rather it depends on the temperature chosen [58]. While we can't accurately estimate all of the interacting complex biological processes that are taking on at the same time, the model functions as an observational model. Activation energy thus should not be thought of as the activation energy utilised in chemical processes, but rather the total temperature response of the microorganism [59].

Even with these problems, the model is in use worldwide. The activation energy, which depends on the temperature change, plays an important role in the metabolic activity of microorganisms, and it has been shown in a variety of conditions not limited to metal-reducing activity and include processes such as the decolorization of various dyes [43,60–63], chromate reduction [49,64] and phenolics biodegradation [38,40,65–67] and molybdenum [44].

The details of the process that causes the change are still unknown, but two hypotheses provide two plausible explanations. The first is that water characteristics change as it transitions and a hypothesis of "bottleneck" hypothesises that a limited number of events occur simultaneously in rapid succession [68]. Based on various measured Arrhenius breakpoint temperatures, the first theory does not seem to be correct [43]. Following the "bottle-neck" idea, since each of the chained enzymes has its unique thermal characteristics, it is impossible to verify the "bottle-neck" hypothesis.

When taking into consideration the ambient temperature, the cell membrane will also vary [69]. The "bottleneck" theory continues to hold strong among academics [43,70]. Alternatively, the Arrhenius plots may be used to estimate the Q_{10} values, or they can be calculated by measuring the rates of growth for different incubation temperatures with ten degrees of variation [71]. When the bioreduction and growth rates have been logarithmically plotted against 1000/temperature (Kelvin), the Arrhenius curve is the slope of the resulting plot (**Fig. 1**).

For the examined temperature range (20-30 °C) and (37-45 °C), Q_{10} values of 2.46 and 3.37 were obtained, respectively. However, since biological processes are dynamic, there may be more than one Q_{10} value for a distinct temperature range being investigated. In the reduction of molybdate to molybdenum blue, a 2.038 value was obtained [72] while in another molybdenum reducer; *Morganella sp.*, a Q_{10} value of 2.31 was obtained. When attributing the growth process to a distinctive biological activity, this value is essential. Q_{10} was calculated to be 2.7 for oil biodegradation in a beach gravel column in previous studies [73]. However, different research on soil polluted with decane and toluene shows a Q_{10} value of 2.2 [74].

Both bacteria's ability to break down petrochemicals and the effects of temperature on it were determined to have a Q_{10} of 2.2 [75], while, immobilised bacterial systems at temperatures ranging from 25 and 45 degrees Celsius produce molybdenum and its Q_{10} value is 2.8. [76]. Increasing the value of Q_{10} as the temperature decreases is often true [77,78]. In another research, *Pseudomonas sp.* strain AQ5-04 produced a Q_{10} value of 1.834 [38] while a Q_{10} value of 2.17 was calculated for the growth rate of this organism on molybdenum. A lower Q_{10} value of 2.17 is reported in another study on molybdenum reduction [44].

For the examined temperature range (20-30 °C) and (37-45 °C), theta values of 1.09 and 1.13 were obtained, respectively (**Fig. 3** and **Fig. 4**), which was similar to a theta value of 1.08 calculated for the molybdenum reduction by the bacterium *Serratia sp.* strain HMY1 [72]. In the growth rate on molybdenum by the Antarctic bacterium *Pseudomonas sp.* strain DRYJ7, a theta value of 1.03 was obtained [44]. The theta value is also within the range for many biological processes that are from 1.1 to 1.7 although higher values of up to 16.2 have been reported for the degradation of other xenobiotics [79].

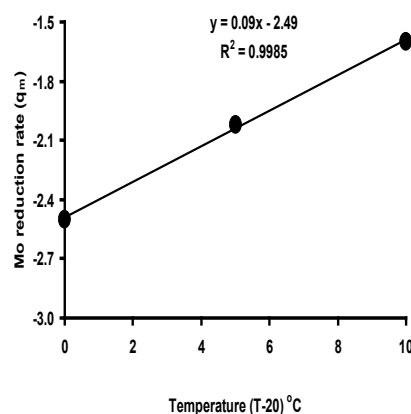


Fig. 3. Estimation of theta value for the rate of Mo-reduction within the temperature range of 20 to 30 °C.

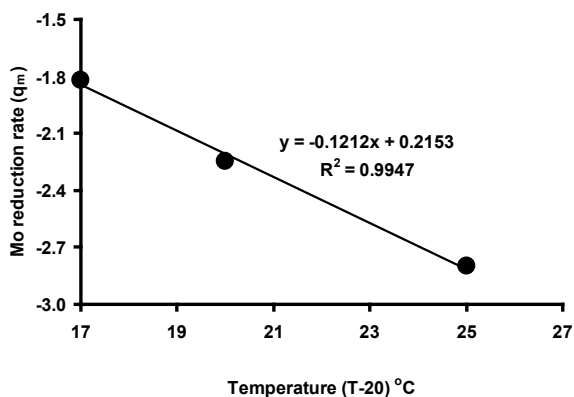


Fig. 4. Estimation of theta value for the rate of Mo-reduction within the temperature range of 37 to 45 °C.

CONCLUSION

This is the first study demonstrated that the activation energy needed for the biodegradation of molybdenum by a bacterium which displays a broken profile with two activation energies observed in the Arrhenius plot. Temperature generally affects microbial growth and metabolic activity on their substrates. The small nature of microbes makes them susceptible to change in the surrounding temperature. Growth on molybdenum by *Acinetobacter calcoaceticus* strain Dr Y12 is described, with a discontinuous chevron-like graph of apparent activation energy with a breakpoint at 32.66 °C. Regression analysis results suggest that in the lower temperature range of 20-30 °C, growth on molybdenum had an activation energy of 66.48 kJ/mol, whereas, at the higher temperature range of 37-45 °C, it had an activation energy of 99.5 kJ/mol. For the examined temperature range (20-30 °C) and (37-45 °C), Q_{10} values of 2.46 and 3.37 and theta values of 1.09 and 1.13 were obtained, respectively. The quantum, especially in between 15 and 20 °C, is relatively a bit higher than the typical energies observed in mesophilic microorganisms. The amide bond is postulated to hold much higher activation energy to be broken. Additional work is under investigation, particularly on parameters themselves, to determine the effects of temperature on growth kinetics. The values obtained in this work are within the normal range for many biological processes. The values obtained in this work are within the normal range for many biological processes.

REFERENCES

- Khan N, Islam MdS. State the organic pollution level in rain fed ponds, Noakhali, Bangladesh. 2019 Aug 5;438-41.
- Karimi-Avargani M, Bazooyar F, Biria D, Zamani A, Skrifvars M. The special effect of the *Aspergillus flavus* and its enzymes on biological degradation of the intact polylactic acid (PLA) and PLA-Jute composite. *Polym Degrad Stab*. 2020 Sep 1;179.
- Tiimub B, Zhenchao Z, Zhu L, Liu Y, Shuai X-Y, Xu L, et al. Characteristics of bacterial community and ARGs profile in engineered goldfish tanks with stresses of sulfanilamide and copper. *Environ Sci Pollut Res*. 2021 Mar 19;1-12.
- Tiimub B, Agyenta J, Azure A, Tiimob G, Osei-Bonsu R. Effectiveness of fluoride decontamination with *Moringa oleifera* and laterite from drinking water resources to safeguard public health at Bongo in Ghana. 2021 Mar 29;6:58-71.
- Stroud J. Coal seam gas (CSG) fracking and extraction in Australia. A spatial human and environmental health risk assessment. [Internet]. [Gold Coast, Australia]: Bond University Australia; 2014 [cited 2021 Jul 15]. Available from: https://www.researchgate.net/publication/299389635_Coal_seam_gas_CSG_fracking_and_extraction_in_Australia_A_spatial_human_and_environmental_health_risk_assessment
- Babalola M, Ayodeji A, Bamidele O, Ajele J. Biochemical characterization of a surfactant-stable keratinase purified from *Proteus vulgaris* EMB-14 grown on low-cost feather meal. *Biotechnol Lett*. 2020 Dec 1;
- Khan N, Islam MdS, Abdul Bari J, Tisha N. Water Quality Evaluation by Monitoring Zooplankton Distribution in Wild Ponds, Noakhali, Bangladesh. *Nat Environ Pollut Technol*. 2020 Dec 3;19:1767-70.
- Omotayo AO, Olagunju KO, Omotoso AB, Ogunniyi AI, Otekinrin OA, Daud AS. Clean water, sanitation and under-five children diarrhea incidence: Empirical evidence from the South Africa's General Household Survey. *Environ Sci Pollut Res Int*. 2021 Jul 5;
- Oksuz A a, Ozyilmaz A a, Aktas M a, Gercek G a, Motte J b. A comparative study on proximate, mineral and fatty acid compositional of deep seawater rose shrimp (*Parapenaeus longirostris*, Lucas 1846) and red shrimp (*Plesionika martia*, A. Milne-Edwards, 1883). *J Anim Vet Adv*. 2009;8(1):183-9.
- Hussain S, Maqbool Z, Ali S, Yasmeen T, Imran M, Mahmood F, et al. Biodecolorization of reactive black-5 by a metal and salt tolerant bacterial strain *Pseudomonas* sp. RA20 isolated from Paharang drain effluents in Pakistan. *Ecotoxicol Environ Saf*. 2013;98:331-8.
- Mohamad Zin N, Mei Chit Y, Abu Bakar NF. Commercial herbal slimming products: Concern for the presence of heavy metals and bacteria. *Pak J Biol Sci*. 2014;17(3):356-63.
- Idris D, Gafasa MA, Ibrahim SS, Babandi A, Shehu D, Ya'u M, et al. *Pantoea* sp. strain HMY-P4 Reduced Toxic Hexavalent Molybdenum to Insoluble Molybdenum Blue. *J Biochem Microbiol Biotechnol*. 2019 Jul 31;7(1):31-7.
- Zhang M, Zhu L, He C, Xu X, Duan Z, Liu S, et al. Adsorption performance and mechanisms of Pb(II), Cd(II), and Mn(II) removal by a β -cyclodextrin derivative. *Environ Sci Pollut Res*. 2019 Feb 1;26(5):5094-110.
- Bose MTJ, Ilavazhahan M, Tamilselvi R, M.Viswanathan. Effect of heavy metals on the histopathology of gills and brain of fresh water fish *Catla catla*. *Biomed Pharmacol J*. 2015 Apr 27;6(1):99-105.
- Asaduzzaman K, Khandaker MU, Binti Baharudin NA, Amin YBM, Farook MS, Bradley DA, et al. Heavy metals in human teeth dentine: A bio-indicator of metals exposure and environmental pollution. *Chemosphere*. 2017;176:221-30.
- Jiang X, Zhou X, Li C, Wan Z, Yao L, Gao P. Adsorption of copper by flocculated *Chlamydomonas microspheara* microalgae and polyaluminium chloride in heavy metal-contaminated water. *J Appl Phycol*. 2019 Apr 1;31(2):1143-51.
- Kai EX, Johari WLW, Habib S, Yasid NA, Ahmad SA, Shukor MY. The growth of the *Rhodococcus* sp. on diesel fuel under the effect of heavy metals and different concentrations of zinc. *Adv Polar Sci*. 2020 May 12;132-6.
- Fathollahi A, Khasteganan N, Coupe SJ, Newman AP. A meta-analysis of metal biosorption by suspended bacteria from three phyla. *Chemosphere*. 2021 Apr 1;268:129290.
- Muliadi FNA, Halmi MIE, Wahid SBA, Gani SSA, Mahmud K, Shukor MYA. Immobilization of Metanil Yellow Decolorizing Mixed Culture FN3 Using Gelling Gum as Matrix for Bioremediation Application. *Sustainability*. 2021 Jan;13(1):36.
- Kovalskiy VV, Yarovaya GA, Shmavonyan DM. Changes of purine metabolism in man and animals under conditions of molybdenum biogeochemical provinces. *Zhurnal Obshchey Biol*. 1961;22(3):179-91.
- Cook GA, Lesperance AL, Bohman VR, Jensen EH. Interrelationship of molybdenum and certain factors to the development of the molybdenum toxicity syndrome. *J Anim Sci*. 1966;25(1):96-101.
- Ward GM. Molybdenum toxicity and hypocuprosis in ruminants: a review. *J Anim Sci*. 1978;46(4):1078-85.
- Abbasi SA. Toxicity of molybdenum and its trace analysis in animal tissues and plants. *Int J Environ Anal Chem*. 1981;10(3-4):305-8.
- Mason J. Thiomolybdates: Mediators of molybdenum toxicity and enzyme inhibitors. *Toxicology*. 1986;42(2-3):99-109.
- Mayr SJ, Mendel R-R, Schwarz G. Molybdenum cofactor biology, evolution and deficiency. *Biochim Biophys Acta BBA - Mol Cell Res*. 2021 Jan 1;1868(1):118883.
- Regoli L, Tilborg WV, Hejjerick D, Stubblefield W, Carey S. The bioconcentration and bioaccumulation factors for molybdenum in

- the aquatic environment from natural environmental concentrations up to the toxicity boundary. *Sci Total Environ*. 2012;435–436:96–106.
27. Zhang Y-L, Liu F-J, Chen X-L, Zhang Z-Q, Shu R-Z, Yu X-L, et al. Dual effects of molybdenum on mouse oocyte quality and ovarian oxidative stress. *Syst Biol Reprod Med*. 2013;59(6):312–8.
 28. Geng C, Gao Y, Li D, Jian X, Hu Q. Contamination investigation and risk assessment of molybdenum on an industrial site in China. *J Geochem Explor*. 2014;144(PB):273–81.
 29. Ojeda AG, Wrobel K, Escobosa ARC, Elguera JCT, Garay-Sevilla ME, Wrobel K. Molybdenum and Copper in Four Varieties of Common Bean (*Phaseolus vulgaris*): New Data of Potential Utility in Designing Healthy Diet for Diabetic Patients. *Biol Trace Elem Res*. 2014;163(1–2):244–54.
 30. Sharma AK, Randhawa SNS, Uppal SK, Ranjan R. Changes in haematology, blood mineral profile, ultra structure and superoxide dismutase activities in erythrocytes in hypophosphatemic buffaloes given excess molybdenum. *Indian J Anim Sci*. 2014;84(5):516–9.
 31. Varun, Sharma S, Sandhu HS, Gosal NS. Haematological profile of subchronic oral toxicity of molybdenum in buffalo calves. *Indian J Anim Sci*. 2014;84(5):520–2.
 32. Al Kuisi M, Al-Hwaiti M, Mashal K, Abed AM. Spatial distribution patterns of molybdenum (Mo) concentrations in potable groundwater in Northern Jordan. *Environ Monit Assess*. 2015;187(3):1–26.
 33. Han MH. Non-linear Arrhenius plots in temperature-dependent kinetic studies of enzyme reactions: I. Single transition processes. *J Theor Biol*. 1972 Jun 1;35(3):543–68.
 34. Ratkowsky DA, Olley J, McMeekin TA, Ball A. Relationship between temperature and growth rate of bacterial cultures. *J Bacteriol*. 1982;149(1):1–5.
 35. McMeekin TA, Chandler RE, Doe PE, Garland CD, Olley J, Putro S, et al. Model for combined effect of temperature and salt concentration/water activity on the growth rate of *Staphylococcus xylosum*. *J Appl Bacteriol*. 1987;62(6):543–50.
 36. Donoso-Bravo A, Bandara WMKRTW, Satoh H, Ruiz-Filippi G. Explicit temperature-based model for anaerobic digestion: Application in domestic wastewater treatment in a UASB reactor. *Bioresour Technol*. 2013;133:437–42.
 37. Mannucci A, Munz G, Mori G, Makinia J, Lubello C, Oleszkiewicz JA. Modeling bioaugmentation with nitrifiers in membrane bioreactors. *Water Sci Technol*. 2015;71(1):15–21.
 38. Aisami A, Yasid NA, Johari WLW, Shukor MY. Estimation of the Q10 value; the temperature coefficient for the growth of *Pseudomonas* sp. aq5-04 on phenol. *Bioremediation Sci Technol Res*. 2017 Jul 31;5(1):24–6.
 39. Shukor MY. Arrhenius Plot Analysis of the Temperature Effect on the Biodegradation Rate of 2-chloro-4-nitrophenol. *Biog J Ilm Biol*. 2020 Dec 30;8(2):219–24.
 40. Onysko KA, Budman HM, Robinson CW. Effect of temperature on the inhibition kinetics of phenol biodegradation by *Pseudomonas putida* Q5. *Biotechnol Bioeng*. 2000 Nov 5;70(3):291–9.
 41. Singh RK, Kumar S, Kumar S, Kumar A. Biodegradation kinetic studies for the removal of p-cresol from wastewater using *Glomastix indicus* MTCC 3869. *Biochem Eng J*. 2008;40(2):293–303.
 42. Reardon KF, Mosteller DC, Bull Rogers JD. Biodegradation kinetics of benzene, toluene, and phenol as single and mixed substrates for *Pseudomonas putida* F 1. *Biotechnol Bioeng*. 2000;69(4):385–400.
 43. Angelova B, Avramova T, Stefanova L, Mutafov S. Temperature effect on bacterial azo bond reduction kinetics: an Arrhenius plot analysis. *Biodegradation*. 2008;19(3):387–393.
 44. Gafar AA, Manogaran M, Yasid NA, Halmi MIE, Shukor MY, Othman AR. Arrhenius plot analysis, temperature coefficient and Q10 value estimation for the effect of temperature on the growth rate on acrylamide by the Antarctic bacterium *Pseudomonas* sp. strain DRYJ7. *J Environ Microbiol Toxicol*. 2019 Jul 31;7(1):27–31.
 45. Zwietering MH, de Koos JT, Hasenack BE, de Witt JC, van't Riet K. Modeling of bacterial growth as a function of temperature. *Appl Environ Microbiol*. 1991 Apr;57(4):1094–101.
 46. Shukor MY, Rahman MF, Suhaili Z, Shamaan NA, Syed MA. Hexavalent molybdenum reduction to Mo-blue by *Acinetobacter calcoaceticus*. *Folia Microbiol (Praha)*. 2010;55(2):137–43.
 47. Arrhenius S. Über die Reaktionsgeschwindigkeit bei der Inversion von Rohrzucker durch Säuren. *Z Für Phys Chem [Internet]*. 1889 Jan 1 [cited 2020 Dec 22]; Available from: <https://www.scienceopen.com/document?vid=f96726d1-41d8-4128-a924-6a2935f01c7a>
 48. Mukerjee-Dhar G, Shimura M, Miyazawa D, Kimbara K, Hatta T. bph genes of the thermophilic PCB degrader, *Bacillus* sp. JF8: characterization of the divergent ring-hydroxylating dioxygenase and hydrolase genes upstream of the Mn-dependent BphC. *Microbiology*. 2005;151(12):4139–4151.
 49. Kavita B, Keharia H. Reduction of hexavalent chromium by *Ochrobactrum intermedium* BCR400 isolated from a chromium-contaminated soil. *3 Biotech*. 2012 Mar;2(1):79–87.
 50. Dey S, Paul AK. Evaluation of chromate reductase activity in the cell-free culture filtrate of *Arthrobacter* sp. SUK 1201 isolated from chromite mine overburden. *Chemosphere*. 2016 Aug 1;156:69–75.
 51. Sallau AB, Inuwa HM, Ibrahim S, Nok AJ. Isolation and properties of chromate reductase from *Aspergillus niger*. *Int J Mod Cell Mol Biol*. 2014;3(1):10–21.
 52. Dhal B, Das NN, Thatoi HN, Pandey BD. Characterizing toxic Cr(VI) contamination in chromite mine overburden dump and its bacterial remediation. *J Hazard Mater*. 2013 Sep 15;260:141–9.
 53. Heerden E van, Opperman DJ, Bester AP, Marwijk JV, Cason ED, Lithauer D, et al. Metabolic promiscuity from the deep subsurface: a story of survival or superiority. In: *Instruments, Methods, and Missions for Astrobiology XI [Internet]*. International Society for Optics and Photonics; 2008 [cited 2020 Dec 23]. p. 70970S. Available from: <https://www.spiedigitallibrary.org/conference-proceedings-of-spie/7097/70970S/Metabolic-promiscuity-from-the-deep-subsurface--a-story-of/10.1117/12.801142.short>
 54. Picard A, Testemale D, Wagenknecht L, Hazael R, Daniel I. Iron reduction by the deep-sea bacterium *Shewanella profunda* LT13a under subsurface pressure and temperature conditions. *Front Microbiol [Internet]*. 2015 [cited 2020 Dec 23];5. Available from: <https://www.frontiersin.org/articles/10.3389/fmicb.2014.00796/full>
 55. Xu X, Xia S, Zhou L, Zhang Z, Rittmann BE. Bioreduction of vanadium (V) in groundwater by autohydrogenotrophic bacteria: Mechanisms and microorganisms. *J Environ Sci*. 2015 Apr 1;30:122–8.
 56. Zhao R, Guo J, Song Y, Chen Z, Lu C, Han Y, et al. Mediated electron transfer efficiencies of Se(IV) bioreduction facilitated by meso-tetrakis (4-sulfonatophenyl) porphyrin. *Int Biodeterior Biodegrad*. 2020 Feb 1;147:104838.
 57. Tchobanoglous G, Schroeder ED. *Water quality: Characteristics, modeling and modification*. 1 edition. Reading, Mass: Pearson; 1985. 780 p.
 58. Ratkowsky DA, Olley J, McMeekin TA, Ball A. Relationship between temperature and growth rate of bacterial cultures. *J Bacteriol*. 1982;149(1):1–5.
 59. Melin ES, Ferguson JF, Puhakka JA. Pentachlorophenol biodegradation kinetics of an oligotrophic fluidized-bed enrichment culture. *Appl Microbiol Biotechnol*. 1997 Jun 1;47(6):675–82.
 60. Chang J-S, Kuo T-S. Kinetics of bacterial decolorization of azo dye with *Escherichia coli* NO3. *Bioresour Technol*. 2000 Nov 1;75(2):107–11.
 61. dos Santos AB, Cervantes FJ, van Lier JB. Azo dye reduction by thermophilic anaerobic granular sludge, and the impact of the redox mediator anthraquinone-2,6-disulfonate (AQDS) on the reductive biochemical transformation. *Appl Microbiol Biotechnol*. 2004 Mar;64(1):62–9.
 62. Dafale N, Wate S, Meshram S, Nandy T. Kinetic study approach of remazol black-B use for the development of two-stage anoxic-oxic reactor for decolorization/biodegradation of azo dyes by activated bacterial consortium. *J Hazard Mater*. 2008 Nov 30;159(2):319–28.
 63. Chen G, Huang M hong, Chen L, Chen D hui. A batch decolorization and kinetic study of Reactive Black 5 by a bacterial strain *Enterobacter* sp. GY-1. *Int Biodeterior Biodegrad*. 2011 Sep 1;65(6):790–6.
 64. Guo J, Lian J, Xu Z, Xi Z, Yang J, Jefferson W, et al. Reduction of Cr(VI) by *Escherichia coli* BL21 in the presence of redox mediators. *Bioresour Technol*. 2012 Nov 1;123:713–6.
 65. Benedek P, Farkas P. Influence of temperature on the reactions of the activated sludge process. In: *Murphy RS, Nyquist D, Neff PW, editors. Proceedings of the international symposium on water*

- pollution control in cold climates. University of Alaska, Washington, DC: Environmental Protection Agency; 1970.
66. Reynolds JH, Middlebrooks EJ, Procella DB. Temperature-toxicity model for oil refinery waste. *J Environ Eng Div.* 1974;100(3):557–576.
 67. Melin ES, Jarvinen KT, Puhakka JA. Effects of temperature on chlorophenol biodegradation kinetics in fluidized-bed reactors with different biomass carriers. *Water Res.* 1998 Jan 1;32(1):81–90.
 68. Kuhn HJ, Cometta S, Fiechter A. Effects of growth temperature on maximal specific growth rate, yield, maintenance, and death rate in glucose-limited continuous culture of the thermophilic *Bacillus caldotenax*. *Eur J Appl Microbiol Biotechnol.* 1980;10(4):303–15.
 69. Ceuterick F, Peeters J, Heremans K, De Smedt H, Olbrechts H. Effect of high pressure, detergents and phospholipase on the break in the arrhenius plot of *Azotobacter nitrogenase*. *Eur J Biochem.* 1978;87(2):401–7.
 70. Mutafov SB, Minkevich IG. Temperature effect on the growth of *Candida utilis* VLM-Y-2332 on ethanol. *Comptes Rendus Acad Bulg Sci.* 1986;39:71–4.
 71. Funamizu N, Takakuwa T. Simulation analysis of operating conditions for a municipal wastewater treatment plant at low temperatures. In: Margesin R, Schinner F, editors. *Biotechnological Applications of Cold-Adapted Organisms* [Internet]. Berlin, Heidelberg: Springer Berlin Heidelberg; 1999 [cited 2019 Jun 15]. p. 203–20. Available from: https://doi.org/10.1007/978-3-642-58607-1_14
 72. Yakasai HM, Yasid NA, Shukor MY. Temperature Coefficient and Q10 Value Estimation for the Growth of Molybdenum-reducing *Serratia* sp. strain HMY1. *Bioremediation Sci Technol Res.* 2018 Dec 31;6(2):22–4.
 73. Gibbs CF, Davis SJ. The rate of microbial degradation of oil in a beach gravel column. *Microb Ecol.* 1976 Mar 1;3(1):55–64.
 74. Malina G, Grotenhuis JTC, Rulkens WH. The effect of temperature on the bioventing of soil contaminated with toluene and decane. *J Soil Contam.* 1999 Jul 1;8(4):455–80.
 75. Oh YS, Kim SJ. Effect of temperature and salinity on the bacterial degradability of petroleum hydrocarbon. *Korean J Microbiol Korea R.* 1989;26(4):339–47.
 76. Kim B-Y, Hyun H-H. Production of acrylamide using immobilized cells of *Rhodococcus rhodochrous* M33. *Biotechnol Bioprocess Eng.* 2002 Aug 1;7(4):194.
 77. Atlas RM, Bartha R. Fate and effects of polluting petroleum in the marine environment. In: Gunther FA, editor. *Residue Reviews*. Springer New York; 1973. p. 49–85. (Residue Reviews).
 78. Deppe U, Richnow H-H, Michaelis W, Antranikian G. Degradation of crude oil by an arctic microbial consortium. *Extrem Life Extreme Cond.* 2005 Dec;9(6):461–70.
 79. Bagi A, Pampanin DM, Brakstad OG, Kommedal R. Estimation of hydrocarbon biodegradation rates in marine environments: A critical review of the Q10 approach. *Mar Environ Res.* 2013 Aug;89:83–90.